

# Cosmology in a petri dish? Simulation of collective dynamics of colloids at fluid interfaces

J. Bleibel<sup>1,2,a</sup>

<sup>1</sup> Max Planck Institute for Intelligent Systems, Heisenbergstr. 3, 70569 Stuttgart

<sup>2</sup> Institute for Theoretical and Applied Physics, University of Stuttgart, Pfaffenwaldring 57, 70569 Stuttgart

**Abstract.** Interfacially trapped, micrometer-sized colloidal particles interact via long-ranged capillary attraction which is analogous to two-dimensional screened Newtonian gravity with the capillary length  $\lambda$  as the tuneable screening length. Using Brownian dynamics simulations and density functional theory, we study the dynamics of an initially prepared distribution of colloids, either a random homogeneous distribution, or a finitely-sized patch of colloids. Whereas the limit  $\lambda \rightarrow \infty$  corresponds to the global collapse of a self-gravitating fluid, for smaller  $\lambda$  the dynamics crosses over to spinodal decomposition showing a coarsening of regions of enhanced density which emerge from initial fluctuations. For the finite patch of colloids and intermediate  $\lambda$  we predict theoretically and observe in simulations a ringlike density peak at the outer rim of the disclike patch, moving as an inbound shock wave. Experimental realizations of this crossover scenario appear to be well possible for colloids trapped at water interfaces and having a radius of around 10 micrometer. Finally, the influence of hydrodynamic interactions on this capillary collapse will be discussed briefly.

## 1 Introduction

Suspensions of colloidal particles serve as model systems for a wide range of problems in physics. Their effective interactions are well understood to that extend, that they may be controlled and used in order to provide tailored model systems for specific physical problems [1]. Additionally, due to the size of the particles in the nano- and micrometer regime, their rich spectrum of physical properties is easily accessible with modern microscopy and imaging technologies.

Of particular interest for the present work are colloidal particles in the micrometer range which are adsorbed at fluid interfaces. Since the trapping process of the particles at the fluid interface is almost irreversible, these colloidal particles form an effectively two dimensional system [1], and provide a convenient frame for the study of statistical mechanics in 2D, both experimentally [2,3] and theoretically [4].

If forces orthogonal to the unperturbed fluid interface are present, the colloidal particles will deform the interface. This deformation gives rise to so-called capillary interactions [5] among the particles, which, in the case of external forces (e.g. gravity) acting on the particles are long-ranged. However, the actual range of the interaction depends on the capillary length  $\lambda$  of the fluid interface [1, 5,4] which depends on the surface tension and opens up the possibility for broad variations of the interaction-range [6]. Therefore, this system provides a rather new model for the study of particles with long-ranged interactions in two dimensions. Depending on the particular setup, it may constitute an analog to screened electrostatics [7] or screened gravitation in 2D [4]. For the latter case interactions may be treated on the mean-field level, providing pairwise-additive interactions among the particles.

---

<sup>a</sup> e-mail: bleibel@is.mpg.de

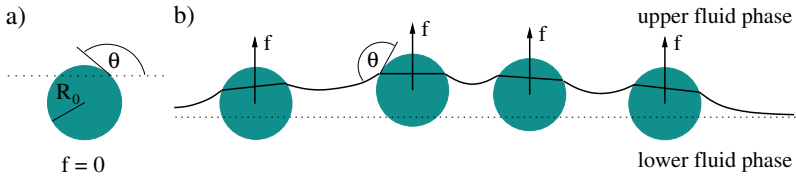


**Fig. 1.** a) A single colloid trapped at a fluid interface (dotted line) without external forces present. b) Identical particles trapped at a fluid interface and deforming it due to external forces  $f$  acting on each of them [4] Upwards pointing forces are taken to be positive. The interface always meets the surfaces of the colloids under a fixed contact angle  $\Theta$ . (Fig. taken from ref. [6])

The system is then well suited for simulations in order to study collective dynamics of 2D systems containing many colloidal particles.

## 2 Theoretical model

The deformation of the interface  $u(x, y)$  may be described by the linearized Young–Laplace Equation:

$$\nabla^2 u - \frac{u}{\lambda^2} = -\frac{1}{\gamma} \Pi \quad (1)$$

where only capillary monopoles contribute to the external pressure  $\Pi = f\delta(\mathbf{r})$ . The surface tension is denoted by  $\gamma$ , whereas  $\lambda$  stands for the capillary length<sup>1</sup>. The solution of equation (1) leads to the pairwise additive potential for two capillary monopoles separated by a distance  $d$  [1,8]:

$$V(d) = -\frac{f^2}{2\pi\gamma} K_0(d/\lambda) \quad (2)$$

with the modified Bessel function  $K_0$ . For length scales much smaller than the capillary length, i.e. large screening lengths of the interaction, this potential is approximately given by

$$V(d) \sim \ln(\lambda/d). \quad (3)$$

Since two monopoles of equal sign always attract each other, equation (3) justifies the use of this system as model for (screened) 2D Newtonian gravity. As a consequence of that, many initial configurations of particles are unstable with respect to a “gravitational” collapse, as in 3D. The colloidal model then constitutes a self gravitating fluid of 2D hard discs<sup>2</sup>. Additionally, this system is highly tunable, as a wide range of length and timescale is accessible. From equation (1) and coarse graining, follows for the mean–field interfacial deformation  $U$ ,

$$\nabla^2 U - \frac{U}{\lambda^2} = -\frac{f}{\gamma} \rho(\mathbf{r}) \quad (4)$$

where we introduced the monopole density  $\rho$ . Upon changing the size and density of the colloidal particles, the value for the capillary monopole  $f$  may be addressed,  $\gamma$  (and thus  $\lambda$ ) may be varied by changing the surface tension. In summary, the system provides an ideal model toolkit for the study of 2D long–ranged interactions.

<sup>1</sup> Note that  $\lambda$  is connected to the surface tension via  $\lambda = \sqrt{\gamma/(g\Delta\rho)}$ , where  $g$  is earth’s acceleration and  $\Delta\rho$  denotes the difference of the densities across the interface

<sup>2</sup> In Brownian dynamics simulations this is usually approximated by more soft discs with a power–law like repelling core.

### 3 Brownian dynamics simulations

#### 3.1 Linear instability of a homogeneous state

We carried out Brownian dynamics (BD) simulations in order to study the collective dynamics of many colloidal particles. Inspired from 3D Newtonian gravity, a linear stability analysis was carried out [4], recovering the Jeans' instability [9] in the limit of infinitely ranged attractive interactions, i.e.  $\lambda \rightarrow \infty$ . Upon defining the Jeans' Wavenumber according to [4]

$$K_j = f \sqrt{\frac{\rho_h p'(\rho_h)}{\gamma}} \quad (5)$$

where  $p(\rho_h)$  denotes the pressure of the 2D discs, and the corresponding Jeans Length via  $L_j = \frac{1}{K_j}$ , we gain a simple criterion to determine the stability for initially homogeneous configurations (characterized by  $\rho_h$ ). The configuration is stable only if  $\lambda K_j < 1$ , otherwise it is unstable. This instability manifests itself in an exponential growth of perturbations with wavenumbers below a critical wavenumber  $k < K_c$ , perturbations with larger wavenumbers are exponentially damped [4]. Furthermore we associate a characteristic timescale with this growth of large scale (small wavenumber) perturbations:

$$\mathcal{T} = \frac{\gamma}{\Gamma f^2 \rho_h} \quad (6)$$

where  $\Gamma$  denotes the mobility of the particles trapped at the interface. Plugging in numbers, we find that for particles of radius  $R_0 = 10\mu\text{m}$  with an initial number density of  $\rho_h = 10^{-2}R_0^{-2}$ , and trapped at an air–water interface ( $\gamma = 72\text{mN/m}$ ) this time is of the order of several hours [4, 6]. The evolution of

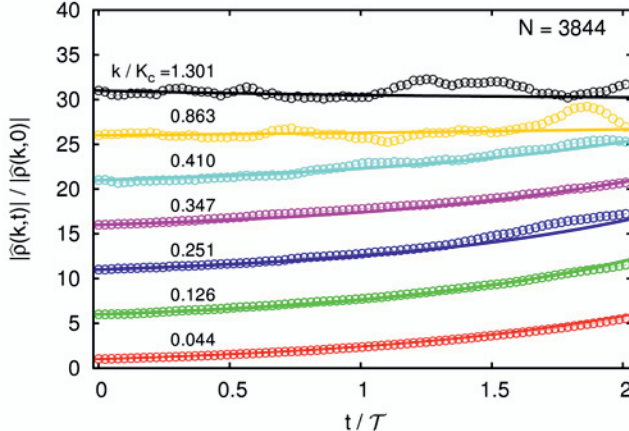


**Fig. 2.** Evolution of Fourier modes of the initial density distribution  $\hat{\rho}(k, t)$  (normalized by the corresponding value for  $t = 0$  and each shifted upwards by 5 for clarity) in a simulation for a  $L \times L$  box,  $L = 620R_0$ , with  $N = 3844$  particles. The error bars concerning the statistical errors, as obtained from averaging within small time intervals of the order of  $\Delta t \approx \mathcal{T}/40$  and over 20 runs of initial configurations, are smaller than the symbol size of the simulation data. The full lines provide the corresponding theoretical prediction for an exponential growth or damping. The figure is taken from ref. [6], where further details of the simulation can be found.

Fourier modes is shown in fig 2, the simulation data agrees nicely with linear stability analysis both for exponential growth and damping up to a time of  $t/\mathcal{T} \sim 1.5$ . As can be seen from simulation snapshots in fig. 3, particles tend to cluster, eventually forming one large cluster at close packing density. This brings up the question how to quantify this clustering dynamics. To do so, we introduce the dynamical

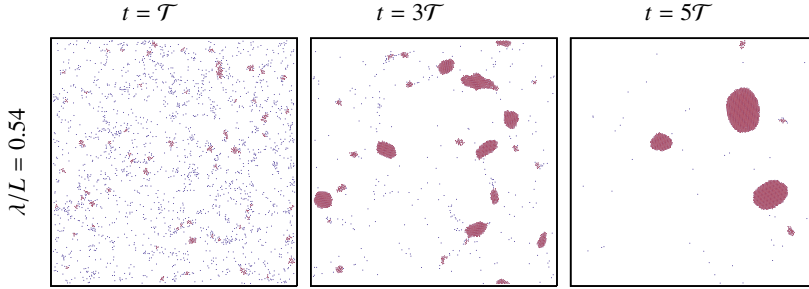


**Fig. 3.** Snapshots of the particle distribution in  $L \times L$  boxes with  $L = 500R_0$  at times  $\mathcal{T}$ ,  $3\mathcal{T}$ , and  $5\mathcal{T}$  for a long-ranged capillary attraction with  $\lambda/L = 0.54$ , corresponding to the usual air–water interface. Clusters (i.e., particles with at least 3 neighbors within a distance of  $3.25R_0$ ) are depicted in red.

quantities of the number of clusters<sup>3</sup>  $n_c$  and the mean cluster size  $S$ . The temporal evolution of these quantities is then studied for different values of the screening length  $\lambda$ , in order to investigate the effect of the range of the interaction on the clustering phenomena. Upon tuning this range parameter, which is also possible for experimental realizations of the system, we are able to establish a smooth connection between systems with a van–der–Waals like short range attraction (and hard core repulsion) and the self gravitating fluid of hard discs corresponding to the very long–ranged limit.

Figure 4 depicts the evolution of the aforementioned dynamical measures of clustering. Two distinct regimes concerning times and values of the range parameter  $\lambda$  can be established. For large  $\lambda$ , one

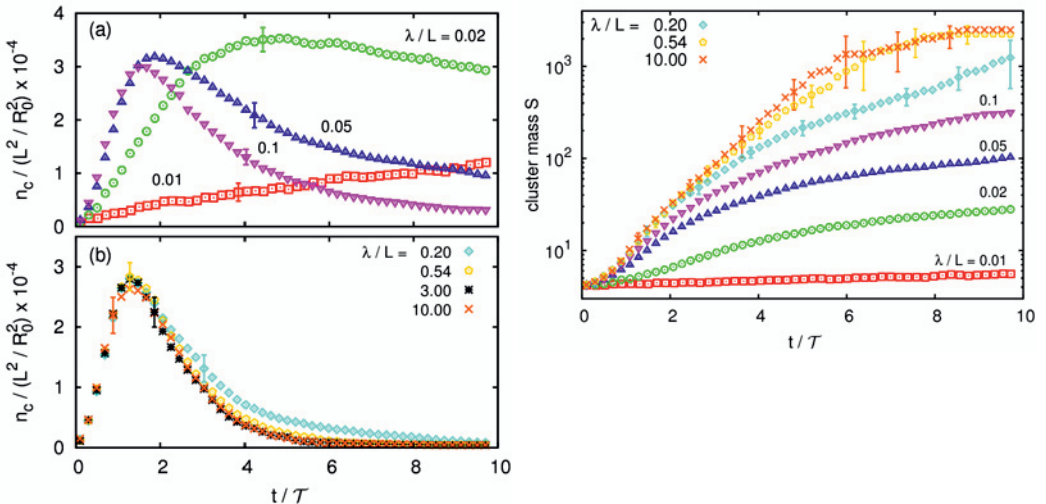


**Fig. 4.** Evolution of the areal number density  $n_c/L^2$  of clusters (left) and the mean cluster mass  $S(t)$  (right) for several values of  $\lambda/L$ , exhibiting the crossover from “short–ranged” attraction (left upper plot (a),  $\lambda \lesssim L$ ) to “long–ranged” attraction (left lower plot (b),  $\lambda \gtrsim L$ ). Only representative error bars are shown, the figures are taken from ref. [6].

observes a rapid clustering up to  $t \simeq 1.5\mathcal{T}$  followed by a rapid domain growth. The evolution scales for  $\lambda \geq 1\text{mm}$  ( $\lambda/L = 0.2$ ), and eventually becomes independent of the latter. The timescale is set by the characteristic time  $\mathcal{T}$  from linear stability analysis, thus one observes the dynamics similar to that

<sup>3</sup> A “cluster” is here defined as a set of more than three particles within a distance of  $d < 3.25R_0$  [6].

of a self gravitating fluid. For small values of  $\lambda$ , however, the maximum is shifted to larger times and no scaling is visible. Since one cannot identify a common characteristic timescale for this subset, we conclude that spinodal decomposition is the governing mechanism of clustering, supported also by a power-law like domain growth (see right panel in fig. 4).

### 3.2 Cold collapse

The cold collapse scenario, i.e. the collapse of a self gravitating, pressureless fluid is a popular standard scenario in the astrophysical literature. Its dynamical evolution can be even solved analytically under certain circumstances. For a so-called top-hat density profile<sup>4</sup> and Newtonian gravity, the radial evolution of an initially radial symmetric density distribution is given by [4]

$$R(t, R_0) = R_0 \sqrt{\frac{\rho}{\rho_h} + \left(1 - \frac{\rho}{\rho_h}\right) e^{t/\mathcal{T}}} \quad (7)$$

and for the time of collapse, where all particles reach the origin, one obtains [6]

$$T_{coll} = -\mathcal{T} \ln \left(1 - \frac{\rho_h}{\bar{\rho}}\right) \quad (8)$$

These equations hold for an infinitely ranged interaction, the shape of the initial profile is then also preserved [4]. In the following this assumption will be relaxed and the cold collapse scenario for the colloidal particles trapped at a fluid interface and interacting via capillary interactions will be investigated. We consider the limit  $\rho_h \rightarrow 0$ , i.e. neglecting any background density, since this seems to be a more natural case for the colloidal particles. For the radial evolution and time of collapse then follows:

$$R(t, R_0) = R_0 \sqrt{1 - \frac{t}{\mathcal{T}}}, \quad T_{coll} = \mathcal{T} \quad (9)$$

We study the evolution of a finite disclike patch of particles for two different initial configurations: First, all particles are arranged in concentric rings, preserving azimuthal symmetry. Brownian motion is switched off. For the second set, these conditions are relaxed: the particles are distributed randomly within the disc and Brownian motion is switched on. Since we expect deviations due to the finite size of the particles and the finite range of the interaction, we modify eq. (9) to account for these changes and introduce [6]:

$$R(t) - R_f = [R_i - R_f] \sqrt{1 - \frac{t}{A_0 \mathcal{T}}} \quad (10)$$

$R_i$  and  $R_f$  denote the initial and final radius of a given ring of particles,  $A_0$  accounts for possible deviations in the time of collapse. As can be seen from fig. 5, the modified radial evolution according to eq. (10) fits the data for all times but the very late stages, where the finite size of the particles comes into play, quite well. The overall deviation for the time of collapse, measured through the  $A_0$  parameter is of the order of 15%.

In order to investigate the origin of this deviation, it is helpful to vary the range parameter of the attraction. Fig. 6 depicts the radial evolution of the outermost ring for three different values of the range parameter  $\lambda$ . As  $\lambda$  grows, the  $A_0$  parameter approaches 1, as expected upon reaching the “Newtonian” limit, i.e.  $\lambda \rightarrow \infty$ . On the other hand, if the range of the interaction decreases,  $A_0$  diverges. It takes more and more time for the distribution to collapse to its equilibrium distribution. In order to shed more light on this regime, various simulations, both for the initial setup with concentric rings and the random distribution of particles, have been carried out for range parameters  $\lambda/L < 1$  (here,  $L$  denotes the initial radius of the collapsing disc).

In fig. 7 we show snapshots of a simulation run for  $N = 1804$  particles and  $\lambda/L = 0.25$ . A ringlike

<sup>4</sup> A top-hat density profile is characterized by a constant background density and a constant overdensity with a certain spatial extent.

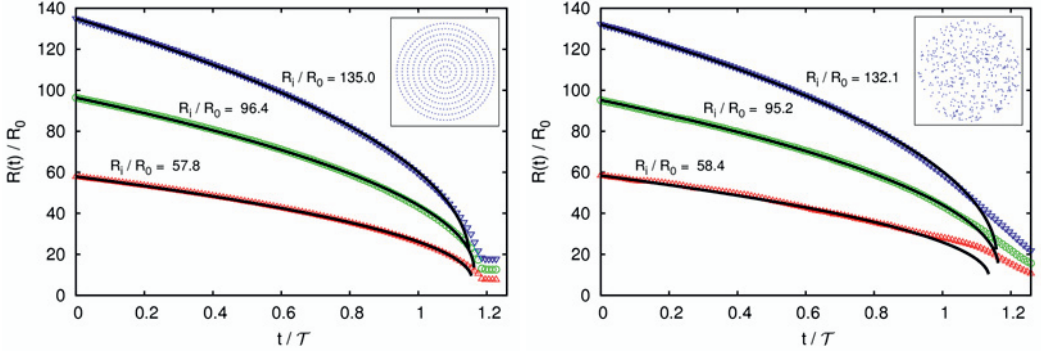


**Fig. 5.** Left panel: Evolution of the radii  $R(t)$  of three rings with initial radius  $R_i/R_0 = R(t = 0)/R_0 = 58, 95$ , and  $135$  for the initial configuration of concentric rings (see inset). The full lines correspond to Eq. (10) with  $(A_0, R_f/R_0) = (1.15, 18), (1.16, 13)$ , and  $(1.16, 8)$  top down. The quadratic simulation box contains initially a disc of radius  $L = 183R_0$ . The number density of particles inside the disc is  $\rho_h = 4.28 \times 10^{-3}R_0^{-2}$ . The range of the capillary attraction is  $\lambda/L = 1.48$ . Right panel: Same as left, but for an initial random distribution of particles (see inset) inside a disc of the same initial radius and with Brownian motion switched on. The radial positions of the particles have been averaged over shells. The full lines correspond to Eq. (10) with  $(A_0, R_f/R_0) = (1.16, 18), (1.16, 13)$ , and  $(1.14, 9)$  from top to bottom. (Figures taken from ref. [6]).

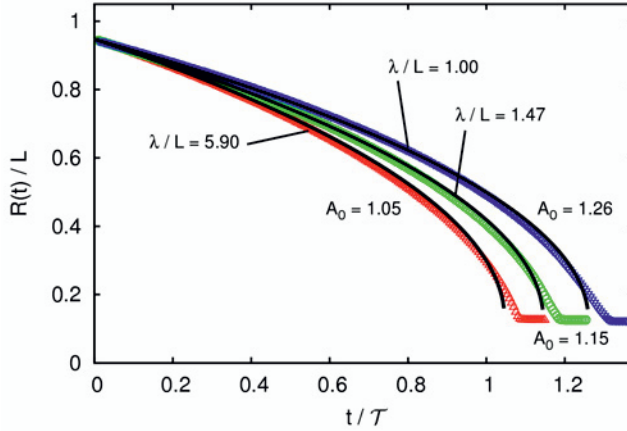


**Fig. 6.** Same as Fig. 5 (left) for the outermost ring ( $R_i/R_0 = 174$ , which is smaller than  $L$  due to binning) for  $\lambda/L = 1, 1.48, 5.9$  and initial disc radius  $L = 183R_0$ . The full lines correspond to the expression in Eq. (10). As expected from Eq. (9) it turns out that  $A_0(\lambda \rightarrow \infty) = 1$ . (Figure taken from ref. [6]).

meta-structure is formed at the outer rim of the initial distribution which slowly moves inward. To investigate this inbound density shockwave more closer, we use the ensemble averaged mean field diffusion equation (mass conservation) for the setup of the collapsing disc [4]:

$$\frac{\partial \rho}{\partial t} = -\nabla(\rho \mathbf{v}) = -\Gamma \nabla(f \rho \nabla U - \nabla p(\rho)). \quad (11)$$

It is convenient to introduce dimensionless variables:

$$\hat{r} = \frac{r}{L}, \quad \hat{\rho} = \frac{\rho}{\rho_0}, \quad \hat{p} = \frac{p}{k_B T \rho_0}, \quad \hat{\lambda} = \frac{\lambda}{L}, \quad \hat{t} = \frac{t}{\mathcal{T}}. \quad (12)$$

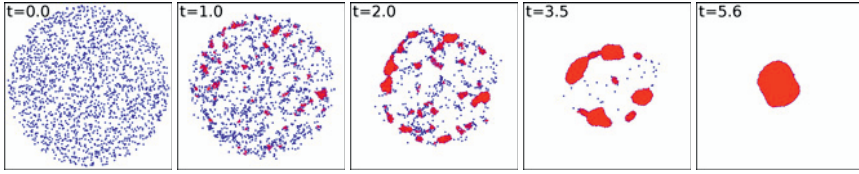


**Fig. 7.** Snapshots from BD simulations for  $\hat{\lambda} = 0.25$ . Small clusters predominantly form at the outer rim and collectively move towards the center. (Figure taken from ref. [10].)

If we further define an effective temperature according to

$$T = \frac{\gamma k_B T}{f^2 \rho_0 L^2}, \quad (13)$$

we can write down the evolution equation for the density [10]:

$$\frac{\partial \hat{\rho}}{\partial \hat{t}} = -\nabla(\hat{\rho} \nabla \hat{U}[\hat{\rho}] - T \nabla \hat{p}(\hat{\rho})) \quad (14)$$

where we used the dimensionless potential of the capillary interaction [10]

$$\hat{U}[\hat{\rho}(\hat{\mathbf{r}})] = 1/(2\pi) \int d\hat{\mathbf{r}}' \hat{\rho}(\hat{\mathbf{r}}') K_0(|\hat{\mathbf{r}} - \hat{\mathbf{r}}'|/\hat{\lambda}). \quad (15)$$

This equation can be viewed as a simple dynamic density functional theory (DDFT) for the collapsing disc. It is expected to hold for scales larger than the particles radius and to correctly describe the collective dynamics of the system [10]. We integrate this evolution equation numerically and compare the result to ensemble averaged data from particle based simulations. As can be seen in fig. 8, the

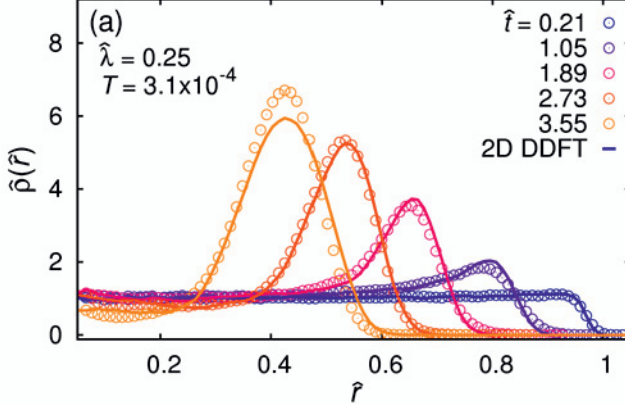


**Fig. 8.** Evolution of the radial density profile for  $T = 3.1 \times 10^{-4}$  and  $\hat{\lambda} = 0.25$ . The colored lines correspond to the 2D-DDFT numerical results, whereas Brownian dynamics simulation data are indicated by symbols (Figure taken from ref. [10]).

DDFT results fit the data from Brownian dynamics simulations for a wide range of times. An inbound moving shockwave is clearly visible. Its existence has also been predicted by an analytical perturbation theory of the cold collapse scenario for finite values of the range parameter [10].

Following the above analysis of the cold collapse scenario, we propose a dynamical phase diagram for a circular patch of particles. The different dynamical regimes are sketched in fig. 9 as a function

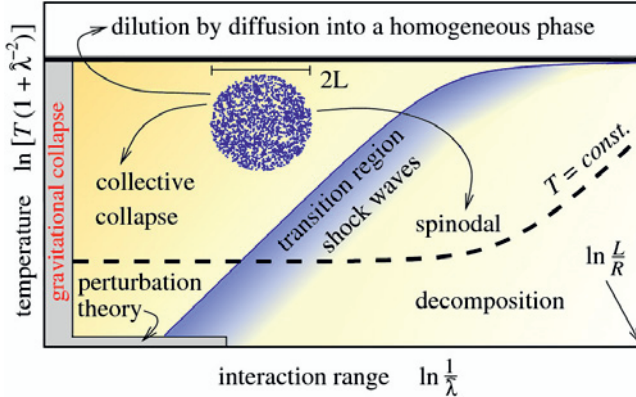


**Fig. 9.** Proposed sketch of dynamical regimes for a circular patch of radius  $L$  with particles of radius  $R$  as function of the range  $\hat{\lambda} = \lambda/L$  of the interaction and a rescaled effective temperature  $T(1 + \hat{\lambda}^{-2})$ .

of the range of the interaction and the rescaled effective temperature  $T(1 + \hat{\lambda}^{-2})$ . The rescaling factor for  $T$  conveniently leads to a horizontal border separating the collapse and dilution regimes [10]. For the collapse, we identify three regimes, however one should note that there is no sharp separating border between them. For  $\lambda/L \rightarrow \infty$  a fast homogeneous collapse is observed. For a finite value of the range parameter in the region  $\lambda/L < 1$ , an inbound traveling shockwave occurs. The time to reach the equilibrium distribution is significantly stretched. Finally, for  $\lambda/L \ll 1$  an individual clustering of the particles dominates the dynamics, consistent with spinodal decomposition and the build up of domains of a characteristic size. The compactification happens only on very long timescales much larger than the characteristic time from linear stability analysis. If the temperature is large enough,  $T(1 + \hat{\lambda}^{-2}) > 1$ , there will be no collapse at all. The distribution will only get diluted.

Since we are discussing particles trapped at a fluid interface and these particles are at least partially immersed in a fluid, the question of hydrodynamics is always at stake. We therefore implemented hydrodynamical interactions<sup>5</sup> (HI) in the Brownian dynamics simulations in order to check the impact on the dynamics. If we compare the evolution of the density profile for  $\hat{\lambda} = 0.1$  for simulations with and without hydrodynamics, as depicted in fig. 10, we find that the shockwave phenomenology

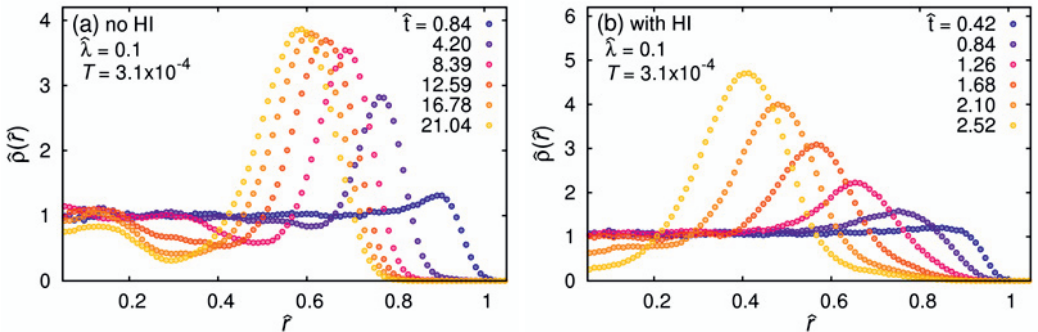


**Fig. 10.** Left panel: Evolution of the radial density profile for  $T = 3.1 \times 10^{-4}$  and  $\hat{\lambda} = 0.1$  without hydrodynamical interactions. Right panel: the same but with HI included.

<sup>5</sup> For an overdamped motion, this can be achieved by relaxing the assumption of a constant mobility and rather using a mobility matrix, here the Rotne–Prager tensor, depending on the positions of all particles.

remains unchanged, however, there is a characteristic change concerning the timescales. The presence of hydrodynamical interactions speeds up the evolution, in this case roughly by a factor of 10.

## 4 Summary and conclusions

In summary, we have investigated the dynamics of colloidal particles which are trapped at a fluid interface and subject to long-ranged capillary interactions. These particles constitute a highly tuneable system, and are thus an ideal toolkit for the investigation of the dynamics of systems with long-ranged interactions. We used Brownian dynamics simulations to study the Jeans' instability of a homogeneous state for colloidal particles at fluid interfaces and confirmed the theoretical prediction from linear stability analysis for the growth and damping of wavelength-dependent perturbations. As the range of the interaction varies from short-ranged to long-ranged, the phenomenology changes from spinodal decomposition to the collapse of a self gravitating fluid. As a second application, we investigated the cold collapse scenario for the colloidal system. In the course of the collapse of a finite circular patch of particles, an inbound traveling shockwave has been theoretically predicted and observed in simulations for intermediate interaction ranges. This led to the invention of a dynamical phase diagram, indicating three different dynamical regimes for the evolution of a circular patch of particles. Whereas for long-ranged interactions a collective collapse similar to the collapse of a self-gravitating fluid is observed, for intermediate interaction ranges and effective temperatures, a shockwave is build up at the outer rim of the distribution, traveling inwards. For short-ranged interactions, the phenomenology further changes to that of spinodal decomposition. We have shown, that the shockwave also shows up in simulations where hydrodynamics are included, only the timescale changes, with an overall speedup of the dynamics.

The author would like to thank his collaborators M. Oettel, A. Domínguez and S. Dietrich, and the DFG for financial support through SFB-TR6 “Colloids in External Fields” (Project N01).

## References

1. M. Oettel, and S. Dietrich, *Langmuir* **24**, 1425 (2008).
2. K. Zahn, J. M. Mendez-Alcaraz, and G. Maret, *Phys. Rev. Lett.* **79**, 175 (1997).
3. K. Zahn, and G. Maret, *Phys. Rev. Lett.* **85**, 3656 (2000).
4. A. Domínguez, M. Oettel, and S. Dietrich, *Phys. Rev. E* **82**, 011402 (2010).
5. P. A. Kralchevsky, and B. N. Naydenov, *Adv. Colloid Interface Sci.* **85**, 145 (2000).
6. J. Bleibel, A. Domínguez, M. Oettel, and S. Dietrich, *Eur. Phys. J. E* **34**, 125 (2011).
7. A. Domínguez, M. Oettel, and S. Dietrich, *J. Chem. Phys.* **108**, 114904 (2008).
8. K. D. Danov, P. A. Kralchevsky, B. N. Naydenov, and G. Brenn, *J. Colloid Interface Sci.* **287**, 121 (2005).
9. J. H. Jeans, *Phil. Transactions of the Royal Society of London Series A*, Vol. **199**, 1 (1902).
10. J. Bleibel, S. Dietrich, A. Domínguez, and M. Oettel, *Phys. Rev. Lett.* **107**, 128302 (2011).